3216 *Chem. Mater.* **2009,** *21,* 3216–3227
DOI:10.1021/cm900810r

CHEMISTRY OF MATERIALS
Article

Spacer-Free Ionic Dye−Polyelectrolyte Complexes: Influence of Molecular Structure on Liquid Crystal Order and Photoinduced Motion

Qian Zhang,[†] Xin Wang,[†] Christopher J. Barrett,[‡] and C. Geraldine Bazuin[*,†]

[†,‡]*Centre de Recherche sur les Matériaux Auto-Assemblés/Centre for Self-Assembled Chemical Structures (CRMAA/CSACS),* [†]*Département de chimie, Université de Montréal, C.P. 6128, succursale Centre-Ville, Montréal, Québec, Canada H3C 3J7, and* [‡]*Department of Chemistry, McGill University, 801 Sherbrooke Street W., Montréal, Québec, Canada H3A 2K6*

Received March 23, 2009. Revised Manuscript Received May 20, 2009

A series of spacer-free ionic azobenzene-containing stoichiometric complexes was prepared from monosulfonated azo dyes and cationic polyelectrolytes [methylated poly(4-vinylpyridine) (PVP) and poly(dimethylaminoethyl methacrylate) (PDM)]. Their thermal and structural characteristics and optical responses, particularly photoinduced birefringence (PIB) and surface relief grating (SRG) inscription, were investigated as a function of selected molecular parameters. All of the complexes have high apparent T_g values, 180−210 °C, and show liquid crystal (LC) order of the single-layer SmA type from ambient to very high temperature, usually to degradation. The range of LC order is greater in the complexes of chromophores with longer alkyl tails and shorter in the complex of the chromophore with an OH end group and the complex of methyl orange (MO) with PDM. PIB, SRG quality, and diffraction efficiency were all shown to depend in a similar way on molecular structural features: the more rigid the molecular structure, the higher the PIB, the better its thermal and temporal stability, and the greater the SRG amplitude. Thus, a flexible alkyl unit in the polyelectrolyte component or in the chromophore tail or spacer reduces the optical performance, with a clear dependence on alkoxy tail length (e.g., no SRG formation was observed for the complex with a hexoxy tail), whereas the most rigid complex, MO/PVP, provides the best performance, contrasting with many previous literature reports that suggest a beneficial role for flexible spacers. The present paper shows that flexible moieties increase relaxation of photoinduced orientation. The hydroxyl end group also provides much improved PIB and SRG performance, attributed to its rigid structure along with a (temperature-dependent) physical cross-linking effect of H-bonding interactions.

Introduction

Azo-containing materials continue to attract considerable interest, particularly in the field of photomechanics,[1] for optoelectronic[2−5] and photochemical[6] applications, as photosensitive molecular machines,[7,8] in life[9,10] and surface[11] sciences, etc. All of these areas take advantage of the well-known azobenzene photoisomerization phenomenon,[12] which allows orientation of the chromophores under irradiation, light triggered changes to shape and polarity etc.[2,5] Many of the azo-containing materials used are in the form of all-covalent polymers.[2] Elements of supramolecular chemistry have also been incorporated into polymeric photonic materials, which can simplify the synthesis and introduce novel properties. For example, Ikeda and colleagues described photobendable films of an azopolymer where hydrogen-bond cross-links replace conventional covalent cross-links.[13] Besides simplifying the preparation of the material, this approach renders it recyclable because of its solubility in suitable solvents in contrast to the insolubility of chemically cross-linked polymers. In another supramolecular system, Ikkala and colleagues demonstrated that enhanced stability and intensity of photoinduced birefringence can be achieved by using hydrogen bonds to bind the chromophore to the polymer chain, allowing high doping levels.[14]

---

*To whom correspondence should be addressed. E-mail: geraldine.bazuin@umontreal.ca.

(1) Barrett, C. J.; Mamiya, J.-i.; Yager, K. G.; Ikeda, T. *Soft Matter* **2007**, 3, 1249–1261. Ikeda, T.; Mamiya, J.-i.; Yu, Y. *Angew. Chem., Int. Ed.* **2007**, 46, 506–528.
(2) Natansohn, A.; Rochon, P. *Chem. Rev.* **2002**, 102, 4139–4175. Natansohn, A.; Rochon, P. *ACS Symp. Ser.* **1997**, 672, 236–250.
(3) Yesodha, S. K.; Pillai, C. K. S.; Tsutsumi, N. *Prog. Polym. Sci.* **2004**, 29, 45–74.
(4) Kucharski, S. H. In *New Research on Optical Materials*; Litchitika, S. J., Ed.; Nova Science Publishers: New York, 2007; pp 119−156.
(5) Kumar, G. S.; Neckers, D. C. *Chem. Rev.* **1989**, 89, 1915–1925.
(6) Peters, M. V.; Stoll, R. S.; Kühn, A.; Hecht, S. *Angew. Chem., Int. Ed.* **2008**, 47, 5968–5972.
(7) Balzani, V.; Credi, A.; Marchioni, F.; Stoddart, J. F. *Chem. Commun.* **2001**, 1860–1861.
(8) Cheetham, A. G.; Hutchings, M. G.; Claridge, T. D. W.; Anderson, H. L. *Angew. Chem., Int. Ed.* **2006**, 45, 1596–1599.
(9) Gorostiza, P.; Isacoff, E. Y. *Science* **2008**, 322, 395–399.
(10) Woolley, G. A. *Acc. Chem. Res.* **2005**, 38, 486–493.
(11) Wang, S.; Song, Y.; Jiang, L. *J. Photochem. Photobiol., C* **2007**, 8, 18–29.
(12) Rau, H. Photoisomerization of azobenzenes. In *Photochemistry and Photophysics*, Rabek, J. K., Ed.; CRC Press: Boca Raton, FL, 1990; Vol. 2, pp 119−141.
(13) Mamiya, J.-i.; Yoshitake, A.; Kondo, M.; Yu, Y.; Ikeda, T. *J. Mater. Chem.* **2008**, 18, 63–65.
(14) Priimagi, A.; Vapaavuori, J.; Rodriguez, F. J.; Faul, C. F. J.; Heino, M. T.; Ikkala, O.; Kauranen, M.; Kaivola, M. *Chem. Mater.* **2008**, 20, 6358–6363. Priimagi, A.; Kaivola, M.; Rodriguez, F. J.; Kauranen, M. *Appl. Phys. Lett.* **2007**, 90, 121103/1–121103/3.

Ionic bonding is another interaction exploited in supramolecular systems for its high strength,[15] such as in dye–surfactant,[16−18] surfactant–polyelectrolyte,[19−22] and surfactomesogen–polyelectrolyte[23−27] complexes, which typically self-assemble into ordered mesomorphous structures. Dye–polyelectrolyte complexes that combine rigidity, liquid crystallinity, and ionic polymer properties as well as high dye loading have been shown to be particularly promising for optical applications.[28−30] In fact, dye–polyelectrolyte systems have been a topic of interest for many years,[15,31] but mainly in solution form,[31−34] as Langmuir–Blodgett films,[35−37] and as layer-by-layer films.[38]

In this paper, we are following up on our communication concerning the simple spacer-free dye–polyelectrolyte complex composed of methyl orange (MO) and methylated poly(4-vinylpyridine) (PVP, where Me is omitted from the acronym for simplicity).[30] This easily prepared material is rigid and possesses liquid crystal (LC) structure up to degradation, and in spin-coated films, it gives high and thermally stable photoinduced birefringence (PIB) and is amenable to surface relief grating (SRG) inscription.[30] Similar properties were reported quasi-simultaneously for a complex of MO with ethylated poly(4-vinyl pyridine).[29a] The exceptional PIB properties were attributed in part to the absence of any flexible spacer or tail in these materials.[30] The role of flexible components in the optical responses of photonic polymers has not yet been well elucidated, and generally chromophores in side chain polymers have been designed with a flexible spacer incorporated, in particular longer ones to promote LC structure that is thought to enhance photo-orientation.[2] The above study suggests that flexible spacers may be counterproductive to optical performances; furthermore, it shows that they are not always necessary for obtaining LC order. In this context, we investigate here a series of mainly spacer-free dye–polyelectrolyte complexes, to examine how certain molecular structural features, and especially the presence of flexible moieties, influence LC order and photoresponsive properties, specifically PIB and SRG inscription. The ease of preparing such complexes is a strong advantage for establishing structure–property relations.

Scheme 1. Chemical Structures of the Complexes Studied[a]

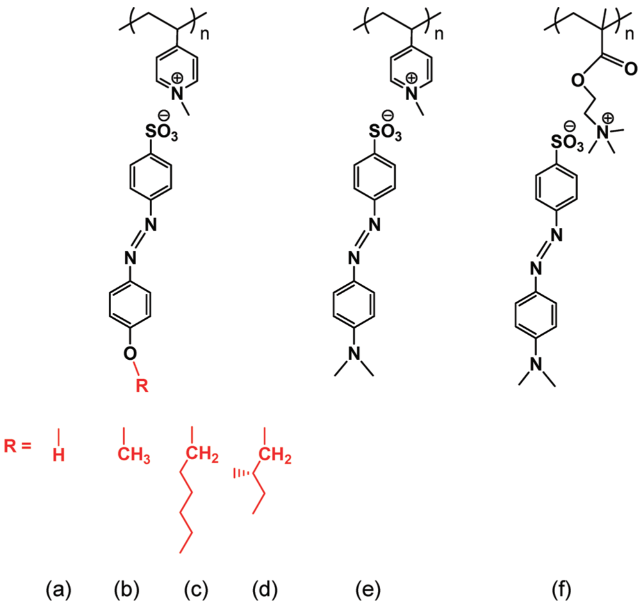

[a] Nomenclature: (a) H/PVP; (b) Me/PVP; (c) Hex/PVP; (d) Ch*/PVP; (e) MO/PVP; and (f) MO/PDM. PVP and PDM refer to the polyelectrolyte components in methylated form (when not complexed, they are designated as PVP-I and PDM-I).

The dye–polyelectrolyte complexes under study are shown, along with the nomenclature used, in Scheme 1. Complexes (a) to (e) have an identical polyelectrolyte backbone, PVP, of relatively high molecular weight. The previously studied complex,[30] MO/PVP (e), serves as a reference. Complexes (a) to (d) differ from (e) by the linking atom (O vs N) between mesogen core and tail and by the tail length and structure. They differ from one another by the tail length [(a) < (b) < (d) < (c)], as well as by a branched tail and therefore chiral center for (d) and by an OH terminal group and therefore hydrogen-bonding capacity for (a). Complex (f) involves MO and a

---

(15) Faul, C. F. J.; Antonietti, M. *Adv. Mater.* **2003**, 15, 673–683.
(16) Everaars, M. D.; Marcelis, A. T. M.; Sudhölter, E. J. R. *Liebigs Ann./Recl.* **1997**, 21–26. Nieuwkerk, A. C.; Marcelis, A. T. M.; Koudijs, A.; Sudhölter, E. J. R. *Liebigs Ann./Recl.* **1997**, 1719–1724.
(17) Stumpe, J.; Goldenberg, L.; Kulikovska, O. Film forming material and preparation of surface relief and optically anisotropic structures by irradiating a film of the said material. WO2006024500, **2006**.
(18) Zakrevskyy, Y.; Stumpe, J.; Faul, C. F. J. *Adv. Mater.* **2006**, 18, 2133–2136. Guan, Y.; Antonietti, M.; Faul, C. F. J. *Langmuir* **2002**, 18, 5939–5945.
(19) MacKnight, W. J.; Ponomarenko, E. A.; Tirrell, D. A. *Acc. Chem. Res.* **1998**, 31, 781–788.
(20) Antonietti, M.; Thünemann, A. *Curr. Opin. Colloid Interface Sci.* **1996**, 1, 667–671.
(21) Zhou, S.; Chu, B. *Adv. Mater.* **2000**, 12, 545–556.
(22) Tsiourvas, D.; Paleos, C. M.; Skoulios, A. *Macromolecules* **1999**, 32, 8059–8065.
(23) Ujiie, S.; Iimura, K. *Macromolecules* **1992**, 25, 3174–3178.
(24) Masson, P.; Guillon, D. *Mol. Cryst. Liq. Cryst.* **2001**, 362, 313–346.
(25) Tibirna, C. M.; Bazuin, C. G. *J. Polym. Sci., Part B: Polym. Phys.* **2005**, 43, 3421–3431. Bazuin, C. G.; Tork, A. *Macromolecules* **1995**, 28, 8877–8880.
(26) Xiao, S.; Lu, X.; Lu, Q.; Su, B. *Macromolecules* **2008**, 41, 3884–3892.
(27) Zhang, Q.; Bazuin, C. G. *Macromolecules*, in press.
(28) Priimagi, A.; Cattaneo, S.; Ras, R. H. A.; Valkama, S.; Ikkala, O.; Kauranen, M. *Chem. Mater.* **2005**, 17, 5798–5802.
(29) (a) Xiao, S.; Lu, X.; Lu, Q. *Macromolecules* **2007**, 40, 7944–7950. (b) Pan, X.; Xiao, S.; Wang, C.; Cai, P.; Lu, X.; Lu, Q. *Opt. Commun.* **2009**, 282, 763–768.
(30) Zhang, Q.; Bazuin, C. G.; Barrett, C. J. *Chem. Mater.* **2008**, 20, 29–31.
(31) Horn, D. *Prog. Colloid Polym. Sci.* **1978**, 65, 251–264.
(32) Goddard, E. D. In *Interactions of Surfactants with Polymers and Proteins*; Goddard, E. D., Ananthapadmanabhan, K. P., Eds.; CRC Press: Boca Raton, 1993; Chapter 4. Lindman, B.; Thalberg, K. In *Interactions of Surfactants with Polymers and Proteins*; Goddard, E. D., Ananthapadmanabhan, K. P., Eds.; CRC Press: Boca Raton, 1993, Chapter 5.
(33) Wang, G.-J.; Engberts, J. B. F. N. *Langmuir* **1994**, 10, 2583–2587.
(34) Abdallah, D.; Cully, M. J.; Li, Y.; Shipp, D. A. *Colloid Polym. Sci.* **2008**, 286, 739–745.
(35) Engelking, J.; Menzel, H. *Thin Solid Films* **1998**, 327–329, 90–95.
(36) Kunitake, T.; Okahata, Y.; Shimomura, M.; Yasunami, S.; Takarabe, K. *J. Am. Chem. Soc.* **1981**, 103, 5401–5413. Tian, Y.; Umemura, J.; Takenaka, T.; Kunitake, T. *Langmuir* **1988**, 4, 1064–1066.
(37) Panambur, G.; Robert, C.; Zhang, Y.; Bazuin, C. G.; Ritcey, A. M. *Langmuir* **2003**, 19, 8859–8866. Panambur, G.; Zhang, Y.; Yesayan, A.; Galstian, T.; Bazuin, C. G.; Ritcey, A. M. *Langmuir* **2004**, 20, 3606–3615.
(38) Advincula, R. C., In *Handbook of Polyelectrolytes and Their Applications*; Tripathy, S. K., Kumar, J., Nalwa, H. S., Eds.; American Scientific: Stevenson Ranch, CA, 2002; Vol. 1, pp 65−97.

Scheme 2. Synthetic Route for the Chromophores[a]

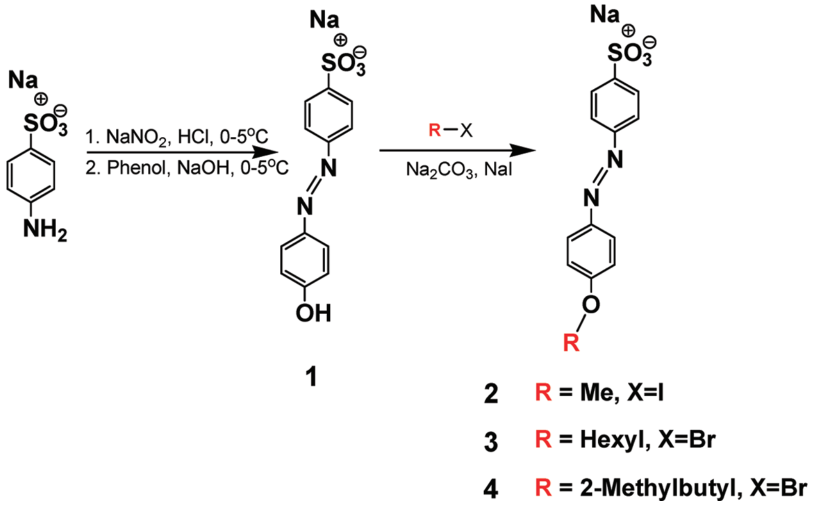

[a] The chromophores are designated by their terminal group (tail) as follows: (**1**) H; (**2**) Me; (**3**) Hex; (**4**) Ch*.

Table 1. Elemental Analysis of the Na^+-Neutralized Chromophores Synthesized and of the Chromophore/Polyelectrolyte Complexes

	C %		H %		N %		S %	
sample	theor.	found	theor.	found	theor.	found	theor.	found
			Chromophore					
H	48.00	48.18	3.02	3.04	9.33	9.32	10.68	11.22
Me	49.68	50.22	3.53	3.48	8.91	8.95	10.20	10.53
Hex	56.24	56.37	5.51	5.46	7.29	7.35	8.34	8.69
Ch*	55.12	54.93	5.17	5.17	7.56	7.71	8.66	8.80
			Complex (+mol H_2O)					
H/PVP + 0.33 H_2O	59.54	59.74	4.91	5.13	10.42	10.36	7.95	8.21
Me/PVP + 0.33 H_2O	60.42	60.41	5.23	5.41	10.07	10.03	7.68	7.92
Hex/PVP + 0.5 H_2O	63.65	63.56	6.57	5.79	8.56	8.37	6.54	6.46
Ch*/PVP + 1.5 H_2O	60.71	60.45	6.52	6.59	8.50	8.36	6.48	6.02
MO/PDM + 1.0 H_2O	55.85	55.88	6.93	6.77	11.33	11.28	6.48	7.16

different polyelectrolyte, methylated poly(dimethylaminoethyl methacrylate) (PDM), which is exempt of aromaticity and contains a short ethylene spacer, making it a more flexible backbone than PVP.

Experimental Section

Materials. Methyl orange was obtained from Sigma-Aldrich and used as received. Poly(4-vinyl pyridine) was obtained from Scientific Polymer Products (viscosity M.W. = 200 000). Poly(*N*,*N*′-dimethylaminoethyl methacrylate) was donated by Prof. R. Jérôme and Dr. C. Detrembleur of the Centre d'Étude et de Recherche sur les Macromolécules (CERM) of Université de Liège, Belgium [SEC (DMF/LiBr; PS standards): $M_n = 16\,600$, $M_w/M_n = 1.22$; true mass estimated at ca. 8000]. Deionized water was obtained from a Millipore Gradient A10 Milli-Q system (resistivity 18.2 MΩ·cm at 25 °C). Spectrograde DMSO (Sigma-Aldrich) was used in the preparation of the complexes.

Synthesis. The Na^+-neutralized chromophores (a) to (d) were synthesized according to Scheme 2, with the details described in the Supporting Information. The H chromophore (**1**) is the precursor compound for the alkoxy-tailed chromophores (**2**−**4**). NMR (given in the Supporting Information) and elemental analysis (Table 1) data indicate highly pure products. Both polymers were quaternized by CH_3I in nitromethane, following literature procedures[30,39,40] and, after precipitation into dichloromethane, were freeze-dried followed by vacuum drying at 40 °C for 3 d. Methylation was verified to be essentially 100% for both polymers by ^1H NMR.

Preparation of Complexes. The procedure for obtaining complexes is similar to that described previously for MO/PVP,[30] except that only a small amount of excess chromophore (relative to stoichiometric) was used because of its poor solubility in water (especially **3** and **4**). A small amount of Milli-Q water was first added to a calculated amount of PVP-I or PDM-I, giving a very viscous solution (~300 mg/mL), to which DMSO (30−40 mg/mL) was then added. Separately, 1.02−1.04 equiv of chromophore was dissolved in DMSO (15 mg/mL). Then, the chromophore solution was added dropwise to the polyelectrolyte solution, giving a transparent orange solution, which was stirred at 55 °C for 6 h. The solution was then transferred to a dialysis bag (SpectraPor, M.W. cutoff 3500; Spectrum Laboratories) and dialyzed against Milli-Q water (refreshed at least daily) for 1−3 weeks to eliminate the Na and I counterions, DMSO, and excess chromophore. The resulting colloidal and/or precipitated mixture was freeze-dried, then further dried under vacuum at 60 °C for 3 d followed by 100 °C for

---

(39) Kawaguchi, D.; Satoh, M. *Macromolecules* **1999**, 32, 7828–7835.

(40) Fang, Z.; Kennedy, J. P. *J. Polym. Sci., Part A: Polym. Chem.* **2002**, 40, 3679–3691.

1 d, and finally stored in a desiccator containing indicator drierite until use. NMR (given in the Supporting Information) and elemental analysis (Table 1) data again indicate highly pure products.

To calculate the stoichiometric ratio of chromophore to the polyelectrolyte repeat unit in the PVP complexes (see ref 30 for MO/PVP), the integration of the protons at the ortho position to the ether link in the chromophores (7.07 ppm generally, 6.92 ppm for H/PVP) was compared to that of the protons at the ortho position to the PVP pyridinium group (broad peak at 9.0−8.3 ppm). For MO/PDM, the integration of the proton at the ortho position to the amino substituent in MO (6.80 ppm) was compared to that of the protons on the ethyl spacer carbon next to the ammonium moiety in PDM (3.81 ppm). The NMR data as well as the elemental analyses (Table 1) indicate highly pure stoichiometric complexes. This is confirmed by EDS which indicated complete elimination of the sodium and iodide counterions.

We verified with the MO/PVP complex that a conventional polymer precipitation technique into water—profiting from the insolubility of the complexes in water—can be employed in place of dialysis to purify the complexes. This is an advantage for preparing larger quantities of complex. To do this, the complex was prepared in solution as for the dialysis procedure, and then the solution was precipitated by dropwise addition into a large quantity of vigorously stirred Milli-Q water. The precipitate was filtered, put in clean Milli-Q water under stirring for a few hours, and then filtered again. This cycle was repeated three times. Finally, the filtered solid was freeze-dried and dried under the same conditions as above. The NMR, EDS, and XRD results for this complex were identical to those of the dialysis-purified complex.

In attempts to obtain recognizable POM textures, thin films were solvent-cast from dilute solutions of the complexes in DMF ($<$ 1% wt) onto clean glass slides. The slides were then covered with a beaker for about 2 weeks to allow very slow solvent evaporation, followed by further drying in vacuum at 80 °C for at least 3 d to eliminate any remaining DMF. Thin films for obtaining UV−visible spectra and for the optical experiments (PIB, SRG) were prepared by spin-coating from a 3/1 DMF/dichloromethane solution (concentration: 3.5 wt % for the films used to obtain UV−visible spectra and 10 wt % for the films used for the optical experiments) onto clean glass slides, which were then vacuum-dried at 100 °C for at least 3 d. The films for the optical experiments were sealed in N_2-flushed polyethylene zipper bags and placed in a Fisher mini-desiccator containing indicator drierite along with a small amount of P_2O_5 for storage and transportation. It is worth mentioning that all of the optical measurements were done in winter months, when the ambient humidity is low.

Instrumentation. Freeze-drying was effected using an FTS Systems FD-3-85A-MP freeze-dryer working at 1−3 mT with the condenser at −90 °C. ^{1}H NMR (500 MHz) spectra were obtained using a Bruker Avance spectrometer. CHNS elemental analysis was performed using a Fisons AE1108 analyzer, Na^+ and Br^- analysis using a FEI Quanta 200 FEG environmental scanning electron microscope equipped with an energy dispersive spectrometer (EDS), and thermogravimetric analysis (TGA) using a TA Instruments Hi-Res TGA 2950 analyzer at a heating rate of 10 °C/min under nitrogen atmosphere. Differential scanning calorimetry (DSC) was performed using a TA Instruments Q2000 DSC at heating and cooling rates of 10 °C/min and polarizing optical microscopy (POM) using a Zeiss Axioskop 40Pol microscope coupled with a Linkam Scientific Instrument THMS600 hot stage and a TMS94 temperature controller. X-ray diffraction (XRD) analysis on powder-like samples packed in 1.0-mm diameter glass capillaries (Charles Supper) was performed with a Bruker D8 Discover system equipped with a 2D Bruker AXS wire-grid detector, using Cu Kα radiation; sample temperature was controlled by a modified Instec HCS410 heating stage and STC200 temperature controller. The acquisition time for each diffractogram was 20−30 min. UV−visible spectra were obtained using a Varian Cary 500 Scan UV−vis−NIR spectrophotometer. A Digital Instruments Dimension 3100 AFM working in tapping mode was used to measure the film thicknesses and to characterize the SRGs. The molecular length was calculated by HyperChem 7.0 (Hypercube), using the MM+ molecular mechanics method, assuming most extended conformations and including van der Waals' radii at the extremities.

The photoinduced birefringence (PIB) experiments were done with the same setup as described elsewhere, except that the pump laser power was much lower in the present experiments.[30,41] The film was placed between two crossed polarizers in an Instec HCS302 hotstage flushed with dry N_2. An Ar ion laser (Spectra-Physics, Model 2030), operated at 488 nm and 320 mW/cm^2 (at this power, no bleaching was observed visually during the experiments) and set at a polarization angle of 45° with respect to the polarizer orientation, was used as the pump laser. A strongly attenuated He−Ne laser (model 1125P; JDS Uniphase), operated at 633 nm and 5.0 mW, was used as the probe laser. Optical erasure was effected using a quarter-wave plate inserted in the path of the pump laser to convert linearly polarized light into circularly polarized light. Photoinduced birefringence values (Δn) were calculated using the equation

$$\frac{I}{I_0} = \sin^2\left(\frac{\pi|\Delta n|d}{\lambda}\right) \tag{1}$$

where I is the photodiode transmission signal, I_0 the photodiode signal in the absence of the sample (parallel polarizer/analyzer orientation), d the film thickness, and λ the probe wavelength.

To measure a series of PIB writing−relaxation−erasure cycles at ambient temperature, the linearly polarized pump laser was turned on for 10 s to obtain birefringence and then turned off for 30 s to observe PIB relaxation. During this relaxation period, a quarter-wave plate was inserted into the optical route of the pump laser to convert it into circular polarization. At the end of the relaxation period, the laser was turned on for 30 s to erase the previously induced birefringence and then turned off for 10 s to allow removal of the quarter-wave plate, after which the next cycle was begun. One PIB writing−relaxation−erasure cycle per temperature was measured at different temperatures during stepwise heating and cooling, all on the same spot (different from the spot used for the room temperature cycles). All of these experiments were done on the same day for all of the complexes except MO/PDM, for which they were done a few days later.

Surface relief gratings (SRGs) were inscribed at ambient temperature using a one-beam setup with a quarter-wave plate and an Ar laser operating at 488 nm (beam diameter enlarged to 15 mm), with the angle between the propagation axis and mirror plane set at approximately 15°. The first order diffraction was tracked with a 633-nm probe laser. This is the same setup as used previously,[30] except that a higher writing power was used in the

---

(41) Natansohn, A.; Rochon, P.; Gosselin, J.; Xie, S. *Macromolecules* **1992**, 25, 2268–2273.

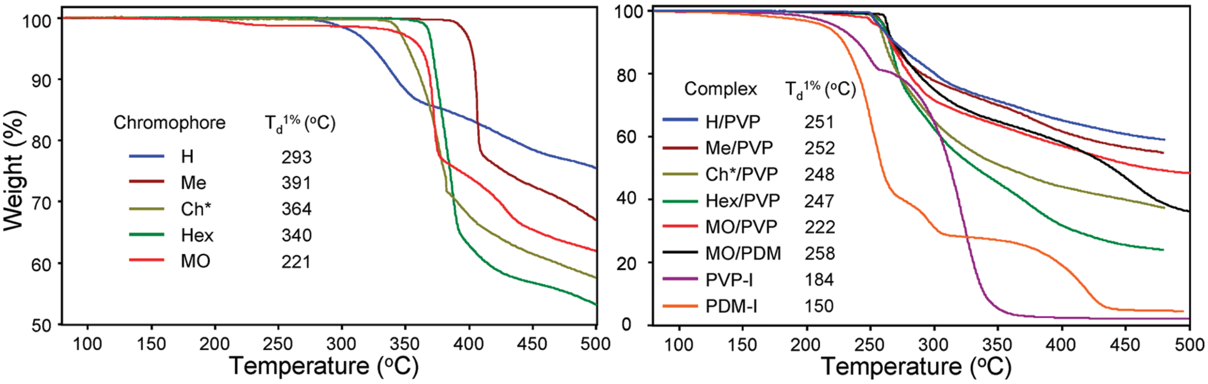

Figure 1. TGA thermograms (left) of the Na^+-neutralized chromophores and (right) of the complexes and I^--neutralized polyelectrolytes.

present experiments, which is more efficient for obtaining high quality SRG patterns.

AFM characterization of the gratings and measurement of film thicknesses were done the day following SRG inscription. The gratings were again examined by AFM about two months later, to check their stability (a mark had been made on the SRGs to ensure inspection of the same region). The same film was used for both PIB and SRG experiments, except for the two MO complexes, for which separate films were prepared. For the films used in PIB experiments, three representative places along scalpel scratches were measured, and the average thickness was used to calculate absolute PIB values using eq 1. For the MO complex films that were used only for SRG, a single place along a scratch very close to the SRG-inscribed area was measured.

Results and Discussion

Thermal and Structural Analysis. The thermal stabilities of the chromophores and complexes were determined by dynamic TGA (Figure 1). The 1% weight losses ($T_d^{1\%}$) of all of the Na^+-neutralized chromophores are above 200 °C, ranging from 220 to 390 °C in the order MO < H < Ch* < Hex < Me. The lower $T_d^{1\%}$ for MO is a result of a small weight loss (2.7%) well before the major loss occurs; this may be related to the dimethylamino terminal group, the only element in this chromophore that differs from the other chromophores. For the complexes, the beginning of major weight loss occurs in a much narrower temperature range (around 250 °C) than for the Na^+-neutralized chromophores and at significantly higher temperatures than for the two I^--neutralized polyelectrolytes.

The synthesized chromophores, like MO, are all crystalline up to decomposition as observed by POM. No peaks were observed in the DSC thermograms (scanned to about 40 °C below $T_d^{1\%}$), except for a broad low-enthalpy one at approximately 210 °C (ca. 200 °C on cooling) for chromophore H. The crystalline character of the chromophores at ambient temperature is confirmed by XRD (Figure 2 and Table 2). For the chromophores with alkoxy terminal groups, the three to four diffraction peaks at lower angles are equidistant, indicating lamellar-type crystalline structures, and their Bragg spacings indicate lamellar thicknesses that are between one and two calculated molecular lengths (Table 2). Chromophore H develops the lowest-angle peak only at high temperature (shown in Figure 2 at 190 °C), to which the low-enthalpy DSC transition may be related.

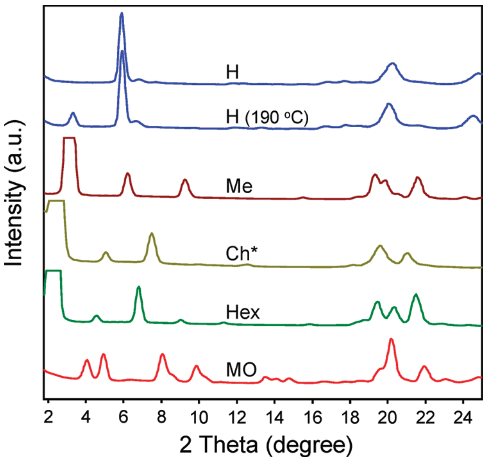

Figure 2. X-ray diffractograms of the Na^+-neutralized chromophores at room temperature (unless otherwise indicated).

Table 2. Bragg Spacings, $d_B(x)$ (x indicating the peak number in order of increasing 2θ), Corresponding to the Lower-Angle X-ray Diffraction Peaks in Figure 2, and the Calculated Molecular Lengths, L_{mol}, of the Na^+-Neutralized Chromophores

chromophore	$d_B(1)$ (Å)	$d_B(2)$ (Å)	$d_B(3)$ (Å)	$d_B(4)$ (Å)	L_{mol}[a] (Å)
H	26.8[b]	14.9			18.5
Me	28.1	14.2	9.5		19.8
Ch*	35.4	17.4	11.8		23.5
Hex	38.8	19.3	13.0	9.8	26.1
MO	21.8	17.8	10.9		20.0

[a] Including sodium (ionic diameter of 1.9 Å). [b] This diffraction peak appeared at temperatures above 190 °C.

The complexes, unsurprisingly, have very different characteristics from the chromophores. Their DSC thermograms are given in Figure 3. In the first heating scan, the complexes show a very broad endotherm (as often observed in initial scans of polymeric materials), with a maximum at about 85 °C for Me/PVP and Ch*/PVP and at about 100 °C for all the others. Otherwise, transitions are observed only above 180 °C. These transitions are relatively broad and, in some cases, their appearance is similar to a glass transition. In others, they appear more like broad peaks, possibly superimposed on a glass-like transition. Because the temperatures above these transitions are fairly close to the onset of degradation (espe-

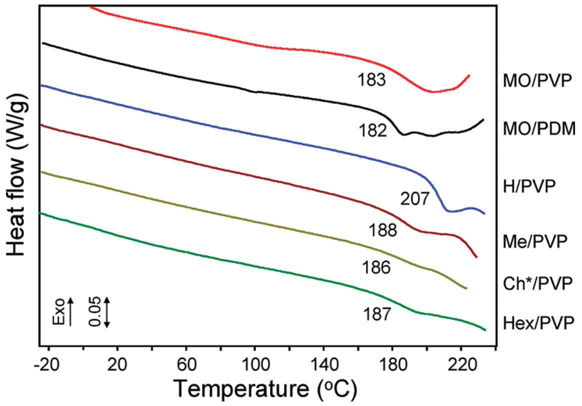

Figure 3. DSC thermograms of the complexes obtained during a second heating scan. The initial heating scan was to a maximum of 200 °C (180 °C for MO/PDM). The high temperature upturn in the MO/PVP thermogram is due to the onset of a sharp, intense exothermic peak related to the onset of degradation.[30] The numbers give the temperature in °C of the inflection point of the initial heat capacity change.[42]

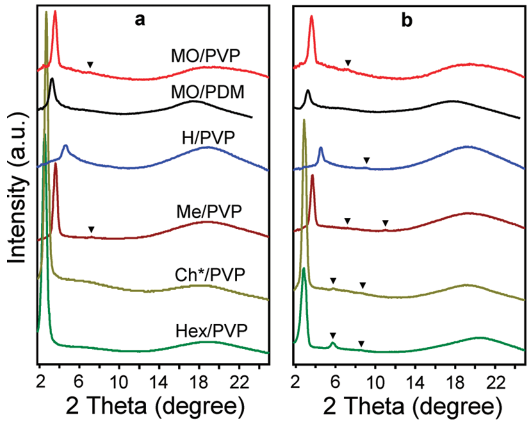

Figure 4. X-ray diffractograms of the complexes (a) at 160 °C (the maximum temperature in the heating–cooling cycle) and (b) at ambient temperature after cooling from 160 °C. Weak higher order diffraction peaks are indicated by arrows.

cially considering that the TGA determinations are dynamic, therefore underestimating degradation onset in conditions involving longer exposure times to high temperature), it is not easy to determine unequivocally the nature of these transitions.

Nevertheless, different pieces of information can be brought to bear in trying to identify them. First, X-ray diffractograms, given in Figure 4 for 160 °C and ambient temperature, show that there is no detectable crystallinity in the complexes (including in the as-prepared samples, for which the diffractograms are almost identical to those in Figure 4b except that the weak peaks marked with arrows are usually less or not at all visible); thus these transitions cannot be melting points. On the other hand, XRD indicates that the complexes have disordered liquid crystal (LC) structure (to be further discussed below), so that the transitions may be a glass transition (which can include an enthalpic peak), an LC–isotropic transition, or an LC–LC transition. POM observations indicate that the complexes with an alkoxy tail are birefringent to temperatures well above the transition (shown in Figure 5 for Hex/PVP), indeed until degradation becomes obvious. At the same time, it was noted that the samples remain powder-like, with no physical deformation possible, until the transition is passed. Above it, the powder-like grains begin to coalesce somewhat, although the material remains highly viscous and hardly spreads under manual pressure. This behavior strongly suggests that the transition is a glass transition in these cases. XRD at high temperature seems to support this assignment, at least for Hex/PVP and Ch*/PVP, for which the small-angle peak in the diffractograms acquired at 230 and 200 °C,[43] respectively, was essentially unchanged from the immediately preceding diffractograms obtained at 160 °C (for Me/PVP, in contrast, this peak in a diffractogram obtained at 210 °C was broadened and much reduced in intensity compared to the preceding 160 °C diffractogram). The resistance to spreading above the transition can be attributed to the strong ionic interactions and high molecular weight of the polymer resulting in a high-modulus rubbery plateau region with low deformability.[44]

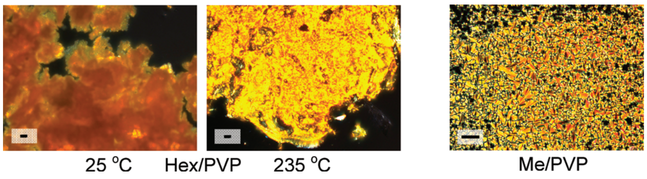

Figure 5. Polarizing optical micrographs for Hex/PVP in powder form at low and high temperature (left pair) and for a solution-cast film of Me/PVP (right). The scale bars represent 20 μm.

For MO/PVP, which is also mechanically rigid and birefringent until degradation, an apparent enthalpy change at approximately 185 °C in its DSC thermogram (reproduced in Figure 3) was assigned tentatively to a glass transition previously.[30] The parallel with the above complexes supports this assignment. The transition region in MO/PDM, which occurs in the same temperature range as MO/PVP, was more difficult to evaluate, particularly because this material had a fluffy rather than powdery aspect and appeared glassy in the microscope, which made any indication of coalescence impossible to see. Birefringence in this complex was much less pronounced than in the alkoxy-tailed complexes. It appeared to decrease slightly in the 190–200 °C region (without increasing again after cooling from that point), but otherwise remained to higher temperatures until degradation set in (as occurred, e.g., after a few minutes at 220 °C). In parallel, an XRD diffractogram obtained at 200 °C showed a broadened low-angle peak compared to lower temperature diffractograms. For H/PVP, clearer birefringence

---

(42) The DSC transition region tends to decrease slightly on each subsequent heating scan, possibly due to a small amount of degradation in the upper temperature range.

(43) In these two cases, a second diffractogram was acquired immediately after the first one at the same two temperatures (each acquisition lasting for 30 min), for which the peak was broadened considerably, reduced in intensity and displaced to lower angles, no doubt a result of degradation.

(44) Ferry, J. D. *Viscoelastic Properties of Polymers*, 3rd ed.; John Wiley & Sons: New York, 1980.

more obviously decreased, but very gradually, as the transition region was crossed (although some residual birefringence remained), and seemed to increase again to a small extent when decreasing the temperature (without any further development of birefringence after annealing, e.g., for a day at 160 °C). The observation that the birefringence is only partly reversible on cooling might be due to the high viscosity of this H-bonding material that restricts growth of mesophase domains (as observed in other ion-containing LC polymer complexes[27,45]) but possibly also to a beginning of degradation, especially considering that the transition region in this case is higher in temperature than for the other complexes (which can be attributed to H-bonding interactions). Although the exact nature of the transition region for H/PVP cannot be pinpointed with certainty, the decrease in birefringence suggests a combination of a glass transition and isotropization, which may account for its appearance as more like a peak compared to the alkoxy-tailed complexes. It is clear, in any case, that all of the complexes have liquid crystalline order up to high temperatures, even up to degradation temperature, as well as very high glass transition temperatures that are hardly affected by the incorporation of flexible tails.

The X-ray diffractograms in Figure 4 illustrate the essentially constant packing structure of the complexes between ambient and high temperature, except that weak higher order peaks are more visible at ambient for most of the complexes. The very high intensity of the first-order peak relative to the wide-angle halo, combined with its narrowness, for Ch*/PVP, Hex/PVP, and, to a lesser extent, for Me/PVP and MO/PVP, is consistent with the high birefringence observed (at high temperatures) in POM for these samples and is indicative of well-developed, long-range LC order. In contrast, H/PVP and MO/PDM have a much weaker and somewhat broader low-angle peak, in accordance with weaker birefringence detected in POM.

As shown in Table 3, the different diffraction order peaks (up to three) are equidistant. This, combined with the absence of wide-angle peaks, is indicative of lamellar packing of the smectic A or C type. The fact that the Bragg spacings determined from these peaks are similar to the calculated molecular lengths (Table 3) favors a single-layer or effective single-layer smectic A assignment, assuming side-by-side ordering of the ionic groups relative to the molecular long axis. This was also concluded previously for MO/PVP, for which a fully interdigitated bilayer structure, resulting in an effective single-layer periodicity, was proposed.[30] This same packing structure appears to apply to all of the complexes investigated.

Table 3. Bragg spaciNgs, $d_B(x)$ (x indicating the peak number in order of increasing 2θ), Corresponding to the Lower-Angle X-ray Diffraction Peaks in Figure 4b, and the Calculated Molecular Lengths, L_{mol}, of the Complexes Investigated

complex	$d_B(1)$ (Å)	$d_B(2)$ (Å)	$d_B(3)$ (Å)	L_{mol}[a] (Å)
H/PVP	19.4	9.8		21.7
Me/PVP	24.0	11.7	8.0	23.9
Ch*/PVP	30.5	15.2	10.1	29.3
Hex/PVP	31.5	15.3	10.2	30.3
MO/PVP	24.2	12.1		23.3
MO/PDM	27.4			25.7

[a] Mesogen and backbone are assumed to be placed side by side relative to the molecular long axis.

It is notable, however, that the Bragg spacings for Ch*/PVP and Hex/PVP increase reversibly with temperature (by 4−5 Å between ambient and the highest temperatures investigated), in contrast to the other complexes for which there is little or no evolution with temperature (see Figure 6). This is frequently associated with smectic C packing,[46] which, however, seems inconsistent with the similarity of the Bragg spacings to the calculated molecular lengths, unless a partially interdigitated tilted bilayer structure (e.g., interdigitated at the level of the alkoxy tails) has a tilt angle that fortuitously results in an apparent single-layer periodicity. It is also notable that, in parallel, the relative intensity of the low-angle peak for Hex/PVP and Ch*/PVP increases significantly (two- and threefold, respectively) and reversibly with temperature between ambient and 160 °C (with still more increase at higher temperatures), whereas this effect is weak for Me/PVP and essentially nonexistent for the other three complexes (see Figure 6). Both phenomena thus appear to be related to the presence of a relatively long alkyl tail. Further clarification of the phase structure details might be obtained from oriented samples; however, the present complexes are not amenable to shearing because of their intractable character up to temperatures dangerously close to degradation onset.

It was previously found that solution-casting followed by slow evaporation of the solvent (DMF) yielded a well-defined focal conic texture for the MO/PVP complex, supporting the identification of its structural order as SmA-like.[30] This technique was also applied to the other complexes. Only Me/PVP gave a well-defined focal conic texture, shown in Figure 4. Unidentifiable textures (possibly ill-defined focal conics) were obtained for Hex/PVP and Ch*/PVP, whereas the texture surprisingly appeared more needle-like for H/PVP (micrographs shown in Supporting Information). MO/PDM showed no birefringence at all.

The thermal and structural order in these complexes may be compared with analogous all-covalent spacer-free side-chain (SC) polymers,[47] a number of which were among the first thermotropic SCLC polymers to be discovered[48,49] before the spacer concept was introduced

---

(45) Vuillaume, P. Y.; Sallenave, X.; Bazuin, C. G. *Macromolecules* **2006**, 39, 8339–8346.

(46) Heinrich, B.; Guillon, D. *Mol. Cryst. Liq. Cryst.* **1995**, 268, 21–43.

(47) Percec, V.; Pugh, C. In *Side Chain Liquid Crystal Polymers*; McArdle, C. B., Ed.; Chapman and Hall: New York, 1989; pp 44−53 and references therein.

(48) Baccaredda, M.; Magagnini, P.; Pizzirani, G.; Giusti, P. *J. Polym. Sci., Polym. Lett. Ed.* **1971**, 9, 303–310. Newman, B. A.; Frosini, V.; Magagnini, P. L. *J. Polym. Sci., Polym. Phys. Ed.* **1975**, 13, 87–93. Frosini, V.; Levita, G.; Lupinacci, D.; Magagnini, P. L. *Mol. Cryst. Liq. Cryst.* **1981**, 66, 341–356.

(49) Blumstein, A.; Hsu, E. C. In *Liquid Crystalline Order in Polymers*, Blumstein, A., Ed.; Academic Press: New York, 1978; Chapter 3.

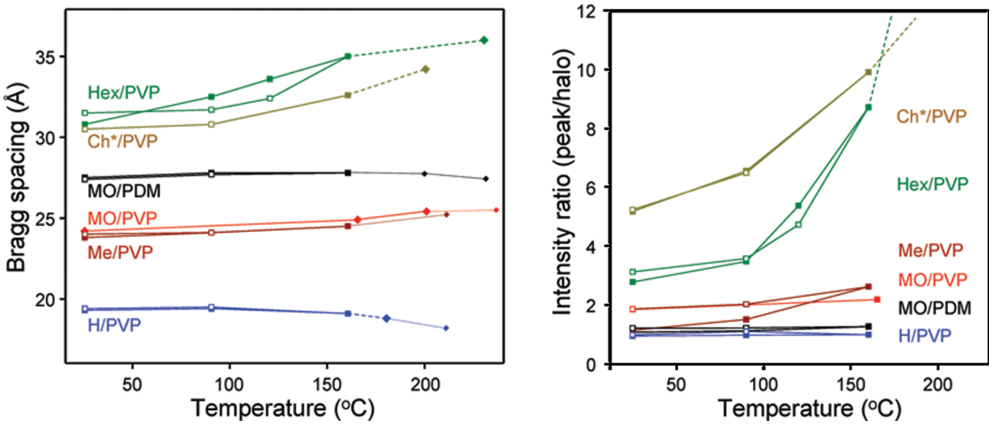

Figure 6. Bragg spacing and intensity (relative to the maximum intensity of the wide-angle halo) of the first order X-ray diffraction peak as a function of temperature for the complexes during heating (closed symbols) and subsequent cooling (open symbols). The temperatures below 160 °C for which only open symbols are visible have closed symbols coincident with the open ones. The points (lozenges) above 160 °C were obtained from a separate set of XRD experiments on samples heated up to degradation, with small lozenges indicating broadened, less intense peaks. The out-of-bound intensity ratios at the end of the dashed lines are 12.6 at 200 °C and 25.3 at 230 °C for Ch*/PVP and Hex/PVP, respectively.

by Finkelmann and colleagues[50] in the late 1970s. In general, spacer-free SCLC polymers, many of them with biphenyl-based rigid cores, are characterized by high T_g values, usually in the 100−200 °C range (but not always detected), and smectic A mesophases that usually either become isotropic above 200 °C (sometimes well above) or are stable to degradation,[47,51] similar to the present complexes (whose apparent T_g values near 200 °C can be attributed to the strong ionic interactions). A study of such polymers based on the phenyl benzoate mesogen with variable length alkoxy tails indicates that both the T_g and the clearing temperature decrease with increase in tail length up to 12 carbons, though both remain very high (180 to 130 and 254 to 208 °C, respectively).[52] The mesophases in the all-covalent polymers are typically bilayer or partially interdigitated bilayer phases,[48,51] in contrast to the effective single-layer phases of the present complexes. It is notable that the insertion of one or two methylene groups between a polyacrylate backbone and a biphenyl side chain converts a smectic A polymer into an amorphous polymer.[53] This can be compared with the somewhat less well-ordered MO/PDM complex compared to the MO/PVP complex (as indicated by weaker birefringence and a less intense low-angle X-ray diffraction peak). It may also be mentioned that a nematic mesophase was reported for a spacer-free side-chain polymer with a carboxylic acid-terminated biphenyl mesogen,[54] which can be correlated perhaps with the weaker LC order observed in the hydrogen-bonding H/PVP complex.

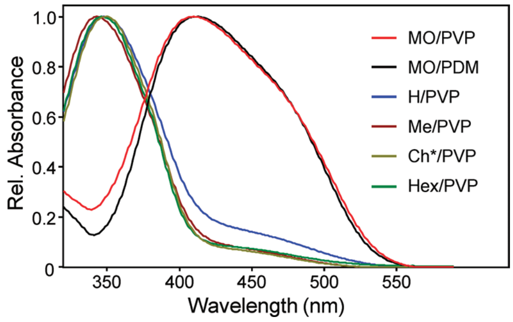

Figure 7. UV−visible spectra of spin-coated films of the complexes.

A series of spacer-free hydrogen-bonded azo complexes with linear alkyl tails ranging from 6 to 10 carbons were similarly ordered into smectic A mesophases, in these cases bilayered with some interdigitation of the alkyl tails.[55] However, the T_g values (ca. 35−60 °C) and isotropization temperatures (ca. 80−125 °C) are much lower than in the present spacer-free ionically bonded azo complexes and in most of the spacer-free all-covalent polymers mentioned above. This illustrates the important role of the ionic interactions in the complexes for obtaining a high-T_g material, even when alkyl tails are present (e.g., Hex/PVP).

Photoinduced Birefringence (PIB). The UV−visible spectra of the spin-coated films are given in Figure 7. The MO complexes show a $\pi-\pi^*$ absorption maximum at 410 nm, along with a distinct shoulder near 480 nm. The maximum is close to that observed for MO in solvents like benzene, dioxane, and acetone.[56] The complexes with the synthesized chromophores show a strong $\pi-\pi^*$ absorption maximum at about 345 nm and a very weak band at about 450 nm that may originate from the

---

(50) Finkelmann, H.; Ringsdorf, H.; Wendorff, J. H. *Makromol. Chem.* **1978**, 179, 273–276.

(51) Alimoglu, A. K.; Ledwith, A.; Gemmell, P. A.; Gray, G. W.; Lacy, F. R. S. D. *Polymer* **1984**, 25, 1342–1346. Duran, R.; Gramain, P.; Guillon, D.; Skoulios, A. *Mol. Cryst. Liq. Cryst., Lett. Sect.* **1986**, 3, 23–31. Duran, R.; Guillon, D.; Gramain, P.; Skoulios, A. *Makromol. Chem., Rapid Commun.* **1987**, 8, 321–324.

(52) Konstantinov, I. I.; Sitnov, A. A.; Grebneva, V. S.; Amerik, Y. B. *Eur. Polym. J.* **1983**, 19, 327–331.

(53) Magagnini, P. L.; Marchetti, A.; Matera, F.; Pizzirani, G.; Turchi, G. *Eur. Polym. J.* **1974**, 10, 585–591. Bresci, B.; Frosini, V.; Lupinacci, D.; Magagnini, P. L. *Makromol. Chem., Rapid Commun.* **1980**, 1, 183–186. Frosini, V.; Levita, G.; Lupinacci, D.; Magagnini, P. L. *Mol. Cryst. Liq. Cryst.* **1981**, 66, 341−356 (21−36).

(54) Blumstein, A.; Blumstein, R. B.; Clough, S. B.; Hsu, E. C. *Macromolecules* **1975**, 8, 73–76.

(55) de Wit, J.; van Ekenstein, G. A.; Polushkin, E.; Kvashnina, K.; Bras, W.; Ikkala, O.; ten Brinke, G. *Macromolecules* **2008**, 41, 4200–4204.

(56) Karukstis, K. K.; Savin, D. A.; Loftus, C. T.; D'Angelo, N. D. *J. Colloid Interface Sci.* **1998**, 203, 157–163.

Table 4. Thicknesses of the Spin-Coated Films and Amplitudes of the Inscribed SRGs, As Measured by AFM

complex	film thickness (nm)	SRG amplitude (nm)
MO/PVP	360,[a] 305[b]	360
MO/PDM	540,[a] 650[b]	305
H/PVP	620[c]	235
Me/PVP	660[c]	75
Ch*/PVP	740[c]	30
Hex/PVP	710[c]	0

[a] Film used for PIB only (three points measured). [b] Film used for SRG only (single point measured). [c] Film used for both PIB and SRG (three points measured).

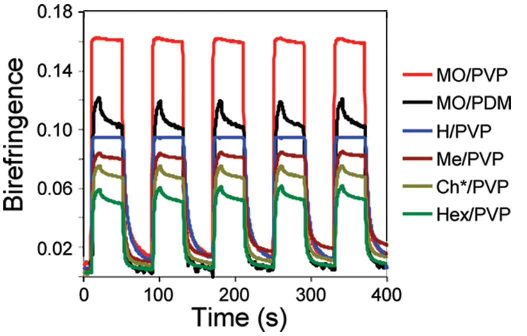

Figure 8. Inscription–relaxation–erasure cycles of photoinduced birefringence (PIB) in spin-coated films of the complexes.

$n \rightarrow \pi^*$ transition, as typical for azobenzene-type molecules.[12]

To evaluate the PIB properties of the complexes, a series of five or more consecutive cycles of writing (linearly polarized laser on for 10 s), relaxation (linearly polarized laser off for 30 s), and erasure (circularly polarized laser on for 30 s, then off for 10 s) were performed at room temperature for each complex. In addition, one writing–relaxation–erasure cycle was performed at each of several other temperatures during step-by-step heating (maximum 180 °C) and cooling. Absolute PIB values were calculated from eq 1 using the film thicknesses determined by AFM (given in Table 4).

The room temperature cycles are shown in Figure 8. Both writing and erasure of PIB is efficient, with good reproducibility, for all of the complexes (except for a slight increase in residual birefringence after erasure, most pronounced for Me/PVP). PIB writing is particularly efficient for MO/PVP and H/PVP. On the other hand, the maximum value of birefringence achieved at the end of the writing period and the relaxation behavior after removal of the writing laser vary from chromophore to chromophore.

To compare directly the PIB performances of the different complexes both at ambient and as a function of temperature, the birefringence at the end of the 10-s writing period (B_1) and the % ratio of the birefringence at the end of the 30-s relaxation period (B_2) to B_1, that is, $B_2/B_1 \times 100$, are plotted against temperature in Figure 9. The maximum temperature tested was 180 °C for all of the complexes except Hex/PVP, which no longer displayed any PIB by 150 °C. The PIB values that were obtained during cooling reproduce those obtained during heating very well, showing excellent reversibility. This reversibility indicates that there is no annealing effect in these complexes, as has been reported for some other photosensitive liquid crystalline polymer films.[29b,57]

In comparing the ambient temperature B_1 values, it is observed that MO/PVP has by far the highest B_1 at 0.16, followed by MO/PDM at 0.12, whereas the complexes with the synthesized chromophores all give a B_1 value of less than 0.1. This is first of all a consequence of the effect of the tail on the chromophore characteristics. In particular, the stronger donor effect of the dimethylamino tail in MO compared to the alkoxy and hydroxyl tails influences B_1 both by modifying the wavelength of maximum absorption relative to that of the writing laser (they are much closer for the MO complexes) and by changing the molecular polarizability. Regarding the latter, high birefringence is related to a high degree of conjugation along the molecular length[58] and consequently a large anisotropy of polarizability.[59,60] For example, Ikeda and colleagues[59] obtained extremely high PIB in an azotolane system, and Atwater and colleagues[61] obtained high birefringence in a diazo system. Generally, stronger donor–acceptor substituents on the azo moiety increase the anisotropy of polarizability.[58] Thus, as indicated by the wavelength of maximum absorption (Figure 7), the two MO complexes can be directly compared to each other, and, separately, the other four complexes can be compared to one another.

To do this, examination of the PIB behavior as a function of temperature is particularly revealing. Comparing the two MO complexes, it is observed that MO/PVP maintains its high B_1 to at least 150 °C with a very small decrease to 0.15 at 180 °C, whereas the B_1 value of MO/PDM decreases strongly with temperature. In parallel, the PIB in MO/PVP shows little or no relaxation, following removal of the writing laser, up to high temperature (B_2/B_1 decreases by only about 5% at 150 °C and less than 20% at 180 °C), whereas MO/PDM shows significant relaxation of PIB even at ambient (nearly 20%) up to more than 50% at 180 °C. It thus appears that the more rigid PVP chain with its aromatic pyridine moiety compared to the more flexible PDM chain with its ethyl spacer and no aromatic unit is advantageous for obtaining high PIB that is stable to high temperatures. Significant PIB relaxation in MO/PDM undoubtedly takes place simultaneously with chromophore orientation during the writing period as well, which can explain

---

(57) Kidowaki, M.; Fujiwara, T.; Morino, S. y.; Ichimura, K.; Stumpe, J. *Appl. Phys. Lett.* **2000**, 76, 1377–1379.

(58) Simpson, S. H.; Richardson, R. M.; Hanna, S. *J. Chem. Phys.* **2007**, 127, 104901/1–104901/14.

(59) Okano, K.; Shishido, A.; Ikeda, T.; Shiono, T. *Mol. Cryst. Liq. Cryst.* **2005**, 441, 275–285. Okano, K.; Shishido, A.; Tsutsumi, O.; Shiono, T.; Ikeda, T. *J. Mater. Chem.* **2005**, 15, 3395–3401. Okano, K.; Shishido, A.; Ikeda, T. *Adv. Mater.* **2006**, 18, 523–527. Okano, K.; Tsutsumi, O.; Shishido, A.; Ikeda, T. *J. Am. Chem. Soc.* **2006**, 128, 15368–15369.

(60) Sekine, C.; Iwakura, K.; Konya, N.; Minai, M.; Fujisawa, K. *Liq. Cryst.* **2001**, 28, 1375–1387.

(61) Lachut, B. L.; Maier, S. A.; Atwater, H. A.; de Dood, M. J. A.; Polman, A.; Hagen, R.; Kostromine, S. *Adv. Mater.* **2004**, 16, 1746–1750.

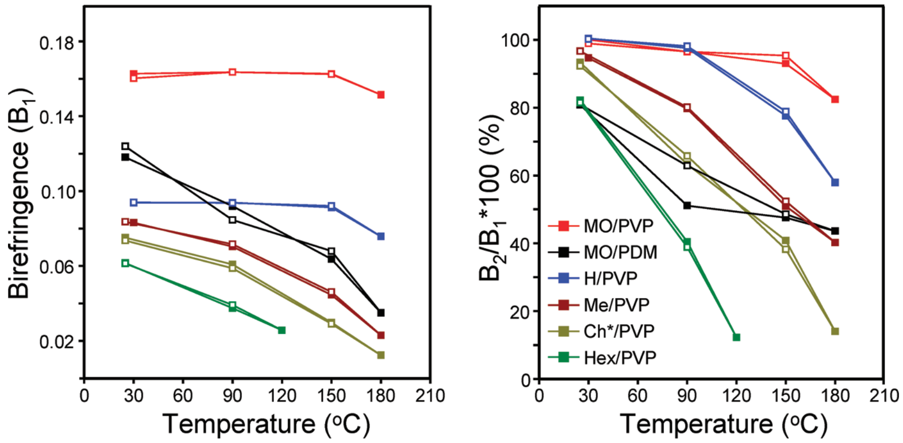

Figure 9. PIB of the different complexes as a function of temperature during heating (closed symbols) and cooling (open symbols): B_1 is the maximum PIB achieved at the end of the 10-s writing period, and B_2 is the birefringence remaining at the end of the 30-s relaxation period. For temperatures where closed symbols are not visible, they are coincident with the open symbols.

its lower B_2 values compared to MO/PVP. This effect is exacerbated on increasing the temperature due to the increasing relaxation in MO/PDM. A complicating factor in comparing the PVP and PDM complexes is the fact that their molecular weights are very different (much lower for PDM), which can also contribute to their differing PIB performance. This is probably attenuated by the fact that their T_g values, as analyzed above, actually appear to be very similar. Nevertheless, by complexing a series of chromophores with systematic structural variations to the *same* polymer, in the present case PVP, any contribution from molecular weight difference is completely eliminated.

The three PVP complexes with alkoxy-tailed chromophores show, like MO/PDM, a decrease in B_1 value and an increase in relaxation (decrease in B_2/B_1) with increase in temperature. The effects are more pronounced in the order Me < Ch* < Hex, which correlates very well with increasing length of the alkoxy moiety, clearly and unequivocally illustrating the deleterious effect of increasing flexibility, this time in the chromophore tail, on high PIB. For Hex/PVP, the relaxation is so pronounced that no PIB at all can be inscribed at 150 °C. The fact that the PIB behavior in Ch*/PVP resembles that in Me/PVP more than that in Hex/PVP, despite its tail length being closer to that of Hex/PVP, can be attributed to the greater bulkiness of the Ch* tail due to the branching on the chiral carbon, which reduces its flexibility somewhat.

The H/PVP complex is an interesting case. Not only is the chromophore free of flexible alkyl moieties, but it possesses an OH tail, which is well-known to lead to hydrogen bonding that can have a (temperature-dependent) physical cross-linking effect. These characteristics can explain why the B_1 values are constant to approximately 150 °C, with a small decrease by about 0.02 units at 180 °C (very similar to MO/PVP). Furthermore, there is little PIB relaxation (B_2/B_1 is approximately constant) up to approximately 90 °C, above which it becomes quite pronounced, with a 40% reduction in B_2/B_1 at 180 °C. A possible reason for the much greater relaxation above 90 °C is that the H-bonds become labile at about 90 °C, thus allowing relaxation to take place, whereas at lower temperatures they prevent relaxation by acting as physical cross-links. During the writing period, in contrast, the B_1 values are constant to a much higher temperature (until 180 °C), which could be related to the kinetics of H-bond exchange being slower than the writing process.

The above results illustrate the importance of minimizing flexible components in the materials to optimize the PIB response. On the other hand, an MO complex with *n*-butylated poly(4-vinyl pyridine) was shown as having no PIB relaxation following removal of the writing laser.[29b] Perhaps the fact that the *n*-butyl group is laterally positioned relative to the long molecular axis of the complex or that it is "isolated" by the rigid aromatic and ionic pyridine moiety that holds the complex together and to which it is attached minimizes its influence.

It is of interest to determine if liquid crystal order influences the PIB. In the series investigated, all of the complexes have LC order, but the extent of this order (correlation length, perfection) varies, as shown above. However, no relationship between the details of liquid crystal order and the PIB behavior is evident. For example, MO/PVP appears to have longer-range LC order and provides superior PIB performance than MO/PDM, whereas the complexes with the alkoxy-tailed chromophores have longer-range LC order but provide inferior PIB performance compared to the OH-tailed complex. Possibly, if LC order has a significant influence on PIB behavior, it is enough that this order exists on a relatively local level, such that the range of order is not a significant factor. It must be kept in mind, also, that the state of order in the spin-coated films is not necessarily the same as in the powder products, something which can be investigated by a technique such as X-ray reflectivity.

Surface Relief Gratings (SRGs). Inscribed surface relief gratings were clearly visible by the naked eye for most of the complexes, suggesting high quality gratings. For Ch*/PVP it was more weakly visible, whereas no evidence of a grating could be found for Hex/PVP. This correlates very well with the AFM observations of the gratings, as described below. An example of an SRG, inscribed on a

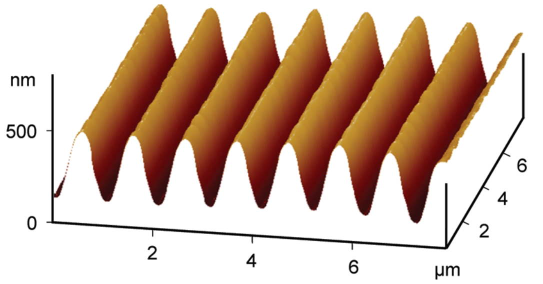

Figure 10. AFM surface profile of an optically inscribed SRG in a spin-coated film of MO/PVP exposed to a linearly polarized 488-nm Ar laser.

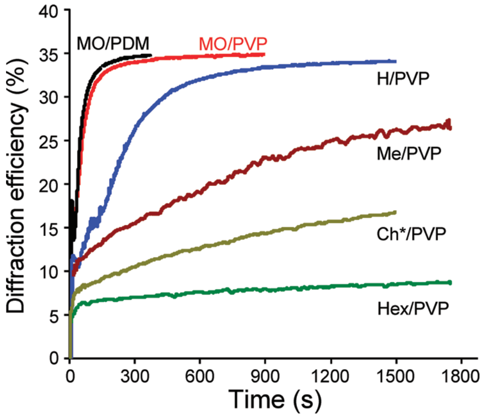

Figure 11. Diffraction efficiency during SRG inscription in spin-coated films of the complexes.

film of MO/PVP and characterized by AFM, is illustrated in Figure 10. The grating is sinusoidal in nature, with a periodicity of 1 μm and an amplitude of 360 nm. The SRGs obtained in the other complexes were also all perfectly sinusoidal with a 1-μm periodicity; only their amplitudes varied, as indicated in Table 4. These amplitudes and the sinusoidal pattern were unchanged when checked again two months later, indicating their high temporal stability (at least at ambient temperature and in a dry atmosphere). No grating was found by AFM for Hex/PVP, consistent with the visual observation. The corresponding diffraction efficiencies for the SRG inscriptions are shown in Figure 11.

Table 4 indicates that the MO complexes have the highest SRG amplitudes and Figure 11 shows that they achieve higher diffraction efficiencies and reach a plateau value more quickly than the other complexes. This may be a consequence, in part, of the greater proximity of the pump laser wavelength (488 nm) to the wavelength of maximum absorption of the MO complex (450 nm) compared to that of the other complexes (~345 nm). However, the MO/PDM complex, whose maximum absorption wavelength is the same as for MO/PVP and whose diffraction efficiency behavior is also very similar, has a significantly lower-amplitude SRG. This can be associated with the greater flexibility of PDM compared to PVP and/or to their molecular weight difference.

When the other complexes, all with a very similar wavelength of maximum absorption and all with the same PVP backbone, are compared, it is observed that the diffraction efficiency curves and the SRG amplitudes follow the same order as the ambient temperature PIB values, thus showing the same dependence on the molecular characteristics of the chromophore tail. It is particularly striking that the hydrogen-bonding tail shows a diffraction efficiency and an SRG amplitude much higher than the alkoxy tail complexes. Indeed, its diffraction efficiency is similar to that of the MO complexes, except that the plateau value is attained more slowly (ca. 20 vs 5 min). In contrast, Hex/PVP shows extremely low diffraction efficiency that may, in fact, be a result of a birefringence grating, since no SRG grating was found. For comparison, it was reported that an octyl perfluorinated tail in a SCLC polymer also prevented SRG formation.[62] It may be added that we attempted to inscribe SRGs in a film of an azo-containing surfactomesogen/polyelectrolyte complex with a 6-carbon spacer [triethyl-6-(4-nitro-azobenzene-4′-oxy)hexylammonium bromide complexed with poly(styrene sulfonate)], which is essentially amorphous and has a T_g of approximately 80 °C.[27] An SRG was visible by eye immediately after writing, but it faded within a few minutes (making this material useful, in fact, for optimizing the optical setup). All of these data indicate that flexible components in the molecular structure of these complexes, whether in the polyelectrolyte constituent or in the chromophore tail or spacer, detract from efficient diffraction and high quality SRGs.

Summarizing Discussion. We had previously shown that the ionic complexation (or ionic self-assembly, ISA[15]) of a commercially available spacer-free ionic dye, methyl orange (MO), with relatively high molecular weight methylated poly(4-vinyl pyridine) (PVP) in stoichiometric proportion leads to a material that remains quite rigid up to degradation, that is characterized by SmA-like liquid crystal packing order, that gives impressively high and thermally stable photoinduced birefringence (PIB), and that is amenable to SRG inscription,[30] similar to a complex of MO with ethylated and *n*-butylated poly(4-vinyl pyridine).[29] Since these supramolecular polymers are quite easy to prepare [including purification by the classical polymer precipitation technique, notably in water (a “green solvent”), although we have preferred a dialysis procedure given the small amounts of sample prepared] and since systematic variants of small molecules like MO are easy to synthesize, they provide ideal systems to investigate the influence of different molecular parameters on their photonic properties. Although various photonic properties have been investigated in many all-covalent azo polymers, a good understanding of structure–property relations is far from complete, with the effect of flexible components and the role of liquid crystallinity still being poorly circumscribed, though some intriguing phenomena have been observed.[2]

In this paper, we have focused on the effect of introducing flexible elements in the ionic chromophore/polyelectrolyte molecular structure, particularly in the

---

(62) Paik, M. Y.; Krishnan, S.; You, F.; Li, X.; Hexemer, A.; Ando, Y.; Kang, S. H.; Fischer, D. A.; Kramer, E. J.; Ober, C. K. *Langmuir* **2007**, 23, 5110–5119.

chromophore tail. These modifications do not affect the overall thermal and structural properties of the complexes. The materials are all mechanically rigid, essentially to degradation, and what are concluded to be T_g values are all similar and very high (ca. 185 °C), with only an OH terminal group on the chromophore causing a mild increase of about 20 °C probably due to H-bonding. They also all display similar lamellar liquid crystal order (appearing to be of the single-layer SmA type) to at least the T_g and usually until degradation, just like MO/PVP. Only the degree of LC order varies somewhat, with longest-range order observed for the complexes with alkoxy tails and the shortest-range order for the complex with the OH tail as well as for the MO complex with methylated poly(dimethylaminoethyl methacrylate) (PDM), which has a short flexible spacer and lacks a rigid aromatic moiety. The lamellar thicknesses are generally invariant with temperature, except for some increase with temperature for the complexes with the longer alkoxy tails (actually reminiscent of tilted lamellar phases, notably SmC), and the long-range order of the latter also reversibly increases with temperature.

On the other hand, the introduction of flexible and other elements in the molecular structure of the complexes strongly influences the photonic properties investigated, far outweighing any potential influence of the details of LC order. In general, both PIB writing and erasure is efficient in the complexes. The highest PIB and the highest amplitude SRGs are obtained with the MO/PVP complex, which is also the most molecularly rigid complex. Its high PIB is maintained to high temperature (with only a small decrease at 180 °C), and in parallel, the PIB relaxation is minimal to more than 150 °C. The substitution of PVP by the more flexible PDM results in significant PIB relaxation that is exacerbated by increasing temperature, with the consequence that the PIB obtained is greatly reduced, along with a reduction in the SRG amplitude (the much lower molecular weight of PDM compared to PVP may also play a role, although this did not change the T_g). The influence of flexible elements is observed more systematically and very clearly in the series of the PVP complexes with the alkoxy tailed chromophores. The longer the alkoxy tail is, the greater the PIB relaxation, the lower the PIB attained, the lower the stability of the PIB with temperature, and the lower the SRG amplitude (with all PIB lost below 150 °C and no SRG at all observed for the complex with the hexoxy tail)—this despite similar, very high T_g values. In contrast, the complex with the hydroxy tailed chromophore shows little PIB relaxation until at least 90 °C and therefore higher PIB that is maintained to high temperature, as well as much higher SRG amplitude, than for the complexes with the alkoxy-tailed chromophores. The increasing PIB relaxation above 90 °C for the former is postulated to be related to H-bond lability having set in. Since little or no PIB relaxation is observed for the MO and OH-tailed complexes with PVP (until high temperature), the PIB that is attained must reflect the maximum PIB possible in the absence of relaxation for the chromophore cores and optical setup and conditions used.

Given the ease of preparation of these kinds of complexes, further improvement of optical performance can be sought, and many other structure−property relations can be determined. To give just a few examples, the effects of ionic cross-linking using disulfonated chromophores or the effects of greater molecular bulkiness and differing molecular shapes using other sulfonated (often commercially available) chromophores can be investigated. Molecular weight effects on both LC and optical properties is also straightforward to study. Comparing the behavior in methylated poly(2-vinyl pyridine) complexes with poly(4-vinyl pyridine) complexes can be of additional interest: although their LC packing structure may be similar,[63,64] their optical properties might be sensitive to the differing molecular placement of the chromophore. Finally, the H/PVP complex described above provides an attractive avenue for manipulating properties that profits from the presence of the OH tail, notably by the addition of (chromophoric) pyridyl derivatives of interest that hydrogen-bond to this tail simultaneously with the ionic complexation.

Conclusions

Azo chromophore−polyelectrolyte ionic complexes not only are potentially useful high-T_g liquid crystalline (LC) optical materials but also provide a relatively simple approach for investigating in detail various relationships between molecular characteristics, packing structure, and optical properties. The present study has focused on the effects of the presence or not of flexible moieties in the chemical structure. It was shown that such moieties have little effect on the T_g and relatively mild effects on the LC structure, affecting mainly the correlation lengths. However, they are clearly detrimental to optimal PIB and SRG performance, largely by allowing relaxation to take place. An interesting temperature-dependent effect from an H-bonding chromophore tail was also found.

Acknowledgment. The financial support of NSERC Canada and FQRNT Québec is gratefully acknowledged. Q.Z. thanks Université de Montréal for a final year graduate scholarship.

Supporting Information Available: Synthesis of the chromophores; NMR data for the chromophores and complexes; high-resolution polarizing optical micrographs of solution-cast complexes (PDF). This material is available free of charge via the Internet at http://pubs.acs.org.

---

(63) Ikkala, O.; Ruokolainen, J.; ten Brinke, G.; Torkkeli, M.; Serimaa, R. *Macromolecules* **1995**, 28, 7088–7094.

(64) Bravo-Grimaldo, E.; Navarro-Rodriguez, D.; Guillon, D. *Macromol. Chem. Phys.* **1997**, 198, 3863–3869.